Development 133, 151-161 doi:10.1242/dev.02174

Identification of multipotent progenitors in the embryonic mouse kidney by a novel colony-forming assay

Kenji Osafune[1,2,3], Minoru Takasato[2,4], Andreas Kispert[5], Makoto Asashima[2,3] and Ryuichi Nishinakamura[1,4,6,*]

Renal stem or progenitor cells with a multilineage differentiation potential remain to be isolated, and the differentiation mechanism of these cell types in kidney development or regeneration processes is unknown. In an attempt to resolve this issue, we set up an in vitro culture system using NIH3T3 cells stably expressing *Wnt4* (3T3Wnt4) as a feeder layer, in which a single renal progenitor in the metanephric mesenchyme forms colonies consisting of several types of epithelial cells that exist in glomeruli and renal tubules. We found that only cells strongly expressing *Sall1* (Sall1-GFP^{high} cells), a zinc-finger nuclear factor essential for kidney development, form colonies, and that they reconstitute a three-dimensional kidney structure in an organ culture setting. We also found that Rac- and JNK-dependent planar cell polarity (PCP) pathways downstream of Wnt4 positively regulate the colony size, and that the JNK pathway is also involved in mesenchymal-to-epithelial transformation of colony-forming progenitors. Thus our colony-forming assay, which identifies multipotent progenitors in the embryonic mouse kidney, can be used for examining mechanisms of renal progenitor differentiation.

KEY WORDS: Progenitor, Kidney, Colony-forming assay, *Sall1*, Wnt, PCP, JNK, Rho, Mouse

INTRODUCTION

Mammalian adult kidney, metanephros, is formed by reciprocally inductive interaction between two precursor tissues derived from the intermediate mesoderm, the metanephric mesenchyme and the ureteric bud. The ureteric bud induces the metanephric mesenchyme to differentiate into the epithelia of glomeruli and renal tubules, endothelial and stromal cells (Saxen, 1987). Inductive signals have been vigorously investigated, and several factors have been elucidated that trigger epithelialization of metanephric mesenchyme in explant culture system; the members of Wnt family (Herzlinger et al., 1994; Kispert et al., 1998), leukemia inhibitory factor (LIF) (Barasch et al., 1999; Plisov et al., 2001), and transforming growth factor β2 (TGFβ2) (Plisov et al., 2001). These studies have also suggested the presence of clonal cells in mesenchymal rudiments, which sequentially form renal condensation, comma (C)- and S-shaped bodies, and terminally epithelia of glomeruli and renal tubules, and the existence of single epithelial precursors responding to LIF was demonstrated in mesenchyme (Barasch et al., 1999). One previous report suggested retrospectively the presence of multipotent cells in embryonic kidneys, demonstrating that cells in several portions of nephron were derived from a single stem cell using *lacZ* gene transduction with retrovirus into a single cell of mesenchyme (Herzlinger et al., 1992). However, none has isolated prospectively the renal progenitor cells with a multilineage differentiation potential from the embryonic kidney, and none has examined their differentiation mechanisms in a single cell culture. There has been a lack of assay systems that specifically identify renal progenitors, as in cases of the neurosphere method for neural stem cells (Reynolds et al., 1992) and the colony assay for hematopoietic progenitors (Pluznik and Sachs, 1965; Bradley and Metcalf, 1966).

We previously generated mice in which the green fluorescence protein gene (*GFP*) was knocked into the locus of *Sall1* (*Sall1-GFP* mice), a zinc finger nuclear factor that is expressed in the metanephric mesenchyme and that is essential for kidney development (Nishinakamura et al., 2001; Takasato et al., 2004). *Sall1* is also expressed in the subventricular zone of the central nervous system and progress zones of limb buds, where neural and mesenchymal stem cells reside, respectively, leading to speculation that *Sall1* might have some association with stem cells in several organs, including the kidney.

Targeted disruption of *Wnt4* results in kidney agenesis and impairs mesenchymal-to-epithelial transformation (Stark et al., 1994), and co-culture with 3T3Wnt4 induces tubulogenesis in the mesenchyme rudiment in organ culture (Kispert et al., 1998), suggesting both essential and sufficient roles of Wnt4 for epithelial differentiation of metanephric mesenchyme. Recently, Wnt9b expressed in the ureteric bud was shown to function upstream of Wnt4 (Carroll et al., 2005). Thus, we attempted to set up assay systems that can identify and characterize the progenitor cells with multipotent differentiation potential from uninduced metanephric mesenchyme using Wnt4 signal. Wnt genes are known to regulate multiple cellular functions using at least three intracellular signaling branches: the β-catenin pathway (canonical pathway), in which stabilized β-catenin interacts with members of the lymphoid enhancer factor/T cell factor (LEF/TCF) family of transcription factors and activates gene expression in the nucleus (Wodarz and Nusse, 1998; Miller et al., 1999); the planar cell polarity (PCP) pathway, which involves Jun N-terminal kinase (JNK) and the Rho family of small guanosine triphosphatases (GTPases) and which directs cytoskeletal rearrangements, coordinated polarization within the plane of epithelial sheets, and morphogenetic movements during development (Veeman et al., 2003; Wallingford et al., 2002); and the Wnt/Ca^{2+} pathway, which leads to release of intracellular calcium and is implicated in *Xenopus* ventralization and in the

[1]Division of Stem Cell Regulation, The Institute of Medical Science, The University of Tokyo, Tokyo 108-8639, Japan. [2]Department of Life Sciences (Biology), Graduate School of Arts and Sciences, The University of Tokyo, Tokyo 153-8902, Japan. [3]ICORP, JST, Saitama 332-0012, Japan. [4]Division of Integrative Cell Biology, Institute of Molecular Embryology and Genetics, Kumamoto University, Kumamoto 860-0811, Japan. [5]Institut für Molekularbiologie, Medizinische Hochschule Hannover, 30625 Hannover, Germany. [6]PRESTO, JST, Saitama 332-0012, Japan.

*Author for correspondence (e-mail: ryuichi@kaiju.medic.kumamoto-u.ac.jp)

Accepted 24 October 2005

regulation of embryonic cell movements (Miller et al., 1999; Veeman et al., 2003; Wallingford et al., 2002). Mechanisms by which Wnt pathways mediate cellular effects in kidney development are poorly understood.

In this study, we established a novel colony-forming assay system using 3T3-expressing Wnt4 to identify renal progenitors in the metanephric mesenchyme. Combining our colony-forming assay with flow cytometry, we found that these progenitors could be enriched by using *Sall1* as a marker. We also examined the effects of Wnt downstream branches on the renal progenitors.

MATERIALS AND METHODS

In vitro colony-forming assay

Metanephric mesenchyme of embryonic day (E) 11.5 mice was isolated surgically from embryonic kidney rudiment. The mesenchyme was incubated in 0.05% trypsin-EDTA at 37°C for 10 minutes and then transferred to DMEM with 10% fetal calf serum. Mesenchymal cells were then mechanically dissociated by gentle aspiration through repeated pipetting. Metanephros of E14.5 and 17.5 embryos was incubated in 1 mg/ml Dispase (Invitrogen) at 37°C for 30 minutes then mechanically dissociated by repeated pipetting. NIH3T3 cells stably expressing Wnt3a, Wnt4 and *lacZ* (Kispert et al., 1998) were mitotically inactivated with mitomycin C before use. Single mesenchymal cells were sorted by FACS Vantage (Becton Dickinson) and plated onto these feeder cells at a low density (5×10^3 cells/well of 6-well plates), then cultured in DMEM/F12 with 5% knockout serum replacement (Invitrogen), 10 μg/ml insulin, 6.7 μg/l sodium selenite, 5.5 μg/ml transferrin, 1×10^{-7} mol/l dexamethasone, 10 mmol/l nicotinamide, 2 mmol/l L-glutamine, 50 μmol/l β-mercaptoethanol, 5 mmol/l HEPES and penicillin/streptomycin.

RT-PCR

Primers used for PCR were as follows:

Pax2, 5′-AGGGCATCTGCGATAATGAC-3′ and 5′-CTCGCGTTTC-CTCTTCTCAC-3′;

Lim1 (*Lhx1* – Mouse Genome Informatics), 5′-TGGACC-GTTTCCTCTTGAAC-3′ and 5′-TGTTCTCTTTGGCGACACTG-3′;

Eya1, 5′-CGGTCGACCTCTATGGAAATGCAGGATCTAAC-3′ and 5′-AACTTCGGTGCCATTGGGAGTC-3′;

Sall1, 5′-TCTCCAGTGTGAGTTCTCTCG-3′ and 5′-GTACACG-TTTCTCCTCAGGAC-3′;

Wt1, 5′-ACCCAGGCTGCAATAAGAGA-3′ and 5′-GCTGAAGG-GCTTTTCACTTG-3′;

Hoxa11, 5′-GGATTTTGATGAGCGTGGTC-3′ and 5′-GAGTAG-CAGTGGGCCAGATT-3′;

glial cell line derived neurotrophic factor (*Gdnf*): 5′-CCCGA-AGATTATCCTGACCA-3′ and 5′-TAGCCCAAACCCAAGTCAGT-3′;

integrin α8, 5′-GGCGAAAGTGCAGTCCTAAA-3′ and 5′-GAAG-GAGACATTCGGAGTGG-3′;

integrin α3, 5′-CGGCCTGTCATCAATATCCT-3′ and 5′-CGAA-CATTGTCCATCAGCAG-3′;

neural cell adhesion molecule (*Ncam*), 5′-ACGTCCGGTTCA-TAGTCCTG-3′ and 5′-CTATGGGTTCCCCATCCTTT-3′;

E-cadherin (cadherin 1 – Mouse Genome Informatics), 5′-GCA-CTCTTCTCCTGGTCCTG-3′ and 5′-GTTGACCGTCCCTTCACAGT-3′;

K-cadherin (cadherin 6 – Mouse Genome Informatics), 5′-CTAGT-GGCTTCCCAGCAAAG-3′ and 5′-CGTGACTTGGACCACAAATG-3′;

Ret, 5′-GCGTCAGGGAGATGGTAAAG-3′ and 5′-CATCAGGG-AAACAGTTGCAG-3′;

Hoxb7, 5′-TTCCCCGAACAAACTTCTTG-3′ and 5′-CGGAGAGG-TTCTGCTCAAAG-3′;

α-actinin-4, 5′-TGGTGCAACTCTCATCTTCG-3′ and 5′-CCGCA-GCTTGTCATACTCAA-3′;

CD2-associating protein (CD2-AP), 5′-AGGAATTCAGCCACAT-CCAC-3′ and 5′-CCTGAGCGTTGTGAGTTTCA-3′;

P-cadherin (cadherin 3 – Mouse Genome Informatics), 5′-CAC-ACGACCTCATGTTCACC-3′ and 5′-GAAATGGTCCCCATCATCAC-3′;

podoplanin, 5′-TCTACTGGCAAGGCACCTCT-3′ and 5′-GCTCTT-TAGGGCGAGACCTT-3′;

podocalyxin-like, 5′-ACTACATTGCCCGTCTCCAC-3′ and 5′-AAA-TCCTCAGCTGGCTTGAA-3′;

aquaporin 1 (*Aqp1*), 5′-CCTCCAGGCACAGTCTTCTC-3′ and 5′-CAGTGGCCTCCTGACTCTTC-3′;

chloride channel 5 (*Clcn5*), 5′-TGGGCTCTTCTGTTTGCTTT-3′ and 5′-GCGAAGAAAGAACGCCATAG-3′;

cubilin (intrinsic factor cobalamin receptor), 5′-CAACCTT-GCCCGTGTTCTAT-3′ and 5′-GTCTGAGTCATCGCTGTGGA-3′;

megalin (low density lipoprotein receptor-related protein 2 – Mouse Genome Informatics), 5′-CAGGGACTCCTCTGACGAAG-3′ and 5′-CCTCTCCTTCTGGACAGTCG-3′;

sodium glucose transporter 1 (*Sglt1*; *Slc5a1* – Mouse Genome Informatics), 5′-GCCATCATCCTCTTCGTCAT-3′ and 5′-ACCACTG-TCCTCCACAAAGG-3′;

Brn1 (*Pou3f3* – Mouse Genome Informatics), 5′-TCTATGGCA-ACGTGTTCTCG-3′ and 5′-CGTCATGCGTTTTTCCTTTT-3′;

Na-K-2Cl co-transporter 2 (*Nkcc2*; *Slc12a1* – Mouse Genome Informatics), 5′-CATGGCATTCATTCTCATCG-3′ and 5′-GCAGAGG-CCACTATTCTTCG-3′;

Clck2 (*Clcnkb* – Mouse Genome Informatics), 5′-CCTCTCA-CTTCTCCGTCTGG-3′ and 5′-AAGAAAGTCCGCTGGCTGTA-3′;

polycystin 2, 5′-GGTGGTGGCAAACTGAACTT-3′ and 5′-TCTC-CAGCTTGACAATCACG-3′;

renal outer medulla K channel 2 (*Romk2*), 5′-TGGTCTCCAAA-GATGGAAGG-3′ and 5′-ATGGCACCACACATGAAAGA3′;

epithelial Na channel (*ENaC*; *Scnn1g* – Mouse Genome Informatics), 5′-GCCTCACTGCTTTCAAGGAC-3′ and 5′-CCAAGTGGGATACT-GGGCTA-3′;

Na/Ca exchanger, 5′-TGTGTTTACGTGGTCCCTGA-3′ and 5′-TGG-AAGCTGGTCTGTCTCCT-3′;

polycystin 1, 5′-CTCTGTGCCCTTCTGAGTCC-3′ and 5′-TGGATCC-ATTCCTTCAAAGC-3′;

Foxd1, 5′-CTGGTGAAGCCTCCCTACTC-3′ and 5′-GCCGTTGTC-GAACATGTCTG-3′; *Flk1* (*Kdr* – Mouse Genome Informatics), 5′-GCATGGAAGAGGATTCTGGA-3′ and 5′-CAAGGACCATCCCAC-TGTCT-3′;

VE-cadherin (cadherin 5 – Mouse Genome Informatics), 5′-ACCGGATGACCAAGTACAGC-3′ and 5′-TTCTGGTTTTCTGGC-AGCTT-3′;

Cd45 (*Ptprc* – Mouse Genome Informatics), 5′-CCACCAGGGACT-GACAAGTT-3′ and 5′-TAGGCTTAGGCGTTTCTGGA-3′; and

glyceraldehyde-3-phosphate dehydrogenase (*Gapdh*), 5′-TGATGA-CATCAAGAAGGTGGTGAAG-3′ and 5′-TCCTTGGAGGCCATGTA-GGCCAT-3′.

PCR cycles were as follows: *Gapdh*, initial denaturation at 94°C for 2.5 minutes, followed by 22 cycles of 94°C for 30 seconds, 60°C for 30 seconds, 72°C for 30 seconds, and final extension at 72°C for 10 minutes; other genes, initial denaturation at 94°C for 2.5 minutes, followed by 28-33 cycles of 94°C for 30 seconds, 58°C for 1 minute, 72°C for 30 seconds, and final extension at 72°C for 10 minutes.

Organ culture

In order to examine the in vitro differentiating potential of cell populations included in the metanephric mesenchyme, each cell population was separated by flow cytometry and was pelleted down by low-speed centrifugation (380 ***g***). The resultant cell pellet (1×10^4 cells per pellet) was cultured on 3T3Wnt4 cells at air-fluid interface on a polycarbonate filter (0.4 μm, Nucleopore) supplied with DMEM plus 10% fetal calf serum at 37°C, 5% carbon dioxide. 3T3Wnt4 cells (50,000 cells in 50 μl medium) were seeded on the filter 24 hours before the experiments, as described (Kispert et al., 1998). To examine the influence of reagents on tubulogenesis, two metanephroi or mesenchyme rudiments from E11.5 embryos were cultured on a polycarbonate filter. For the culture of mesenchyme rudiments, 3T3Wnt4 cells were used as described above.

Retroviral infection

The cDNA clones of the active mutant form of β-catenin (*pUC-EF-1α-β-catenin^{SA}-3HA*) (Miyagishi et al., 2000), the full length of rat axin (*pBSKS-rAxin*) (Ikeda et al., 1998), and both constitutively-active and dominant-negative mutant forms of human *Rac1* and *RhoA* with N-terminus flag tag [*pCAGIP-flag-Rac1 (Val)*, *pCAGIP-flag-Rac1 (Asn)*, *pCAGIP-flag-RhoA (Val)*, *pCAGIP-flag-RhoA (Asn)*] were subcloned into retroviral vector *pMY-IRES-EGFP* (Kitamura et al., 2003). To produce recombinant retrovirus, these plasmid vectors were transfected into the virus packaging cell line PLAT-E (Morita et al., 2000) using FuGENE (Roche), and supernatant from the transfected cells was collected to infect cells of the metanephric mesenchyme. The viral supernatant was centrifuged at 20,000 ***g*** overnight at 4°C to concentrate the virus. To infect mesenchymal cells with the retrovirus, dissociated mesenchymal cells were resuspended into the concentrated virus supernatant with adding polybrene. The suspension was centrifuged 1400 ***g*** for 4 hours at room temperature. After washing with PBS, mesenchymal cells were plated onto 3T3 feeder cells.

Immunocytochemistry and lectin staining

The colonies formed on 3T3Wnt4 feeder were fixed with 4% paraformaldehyde in PBS for 20 minutes at 4°C. After washing with PBS, PBS containing 2% skimmed milk and 0.1% Triton-X was incubated as a blocking solution for 1 hour at room temperature. The fixed dishes were incubated with primary antibodies overnight at 4°C followed by incubating with secondary antibodies for 1 hour at room temperature. The following antibodies were used: rabbit anti-Pax2 (Babco), rabbit anti-WT1 (Santa Cruz), mouse anti-E-cadherin (Becton Dickinson), rabbit anti-AQP1 (Chemicon), and rabbit anti-phosphorylated JNK1 and 2 (Biosource). Rhodamine-conjugated anti-rabbit IgG (H+L) and anti-mouse IgG (Chemicon) were used as secondary antibodies. To examine the expression of a proximal renal tubule-specific marker, fluorescein isothiocyanate (FITC)-conjugated *Lotus Tetragonobulus* lectin (LTL; Vector Labs) was used. After each step, the cultured cells were washed three times with PBS containing 0.1% Triton-X. For detection of Sall1, mesenchymal cells derived from *Sall1-GFP* heterozygote embryos were cultured on 3T3 feeder and subjected to GFP immunostaining procedure using rabbit anti-GFP (Molecular Probes). Rhodamine-conjugated peanut agglutinin (PNA; Vector Labs) staining was done as described (Gilbert et al., 1994). Organ culture tissues were fixed with 4% paraformaldehyde in PBS for 1 hour at 4°C and incubated in PBS including 0.1% saponin (Sigma) for 1 hour at 37°C, then the same staining procedure was carried out. Staining with rabbit anti-secreted frizzled-related protein 2 (sFRP2; Santa Cruz) and FITC-conjugated *Dolichos biflorus* agglutinin (DBA; Vector Labs) were also used on sections of paraffin-embedded explants to examine the effect of reagents on tubule formation and branching, respectively.

RESULTS

In vitro colony formation from E11.5 metanephric mesenchyme

We cultured single cells from the metanephric mesenchyme of E11.5 embryos, using 3T3Wnt4 as a feeder layer in a serum-free condition. The metanephric mesenchyme of transgenic mice ubiquitously expressing enhanced green fluorescence protein (EGFP; Okabe et al., 1997) was used to distinguish mesenchyme-derived cells from feeder cells, and single cells sorted by flow cytometry were cultured at a low cell density on 3T3Wnt4. This culture condition resulted in the formation of sheet-like colonies not formed on 3T3*lacZ* (Fig. 1A, upper panels), while scattered fibroblast-like cells were observed in both conditions (Fig. 1A, lower panels, arrows). Colonies were not formed in the presence of frizzled (Fz)-Fc chimeric protein, a Wnt inhibitor, thus confirming an essential role of Wnt4 for colony formation (Fig. 1B). Colonies were not formed by culturing in the conditioned medium from 3T3Wnt4 without feeder cells (data not shown). Colonies were also formed on 3T3Wnt3a, but not in feeder-free conditions using a purified recombinant Wnt3a protein (data not shown). These data suggested the requirement of other signals from 3T3 cells, in addition to the Wnt signals for the colony formation. In the presence of serum, colonies were not formed even on 3T3Wnt4, and some factors in the serum might prevent colony formation (data not shown). When colonies on 3T3Wnt4 were dissociated and plated onto fresh feeder cells at day 10 of culture, few colonies were obtained, and maintenance of these colonies could not be achieved (data not shown). When we tried colony-formation by using polycarbonate filters, which separate mesenchymal cells from the feeder layer, colonies were formed but the number of colonies formed was much smaller than that formed by directly culturing on feeder cells (data not shown).

To characterize the molecular profiles of the colonies, genes expressed in the metanephric mesenchyme were examined by RT-PCR using RNA from the colonies together with 3T3Wnt4 (Fig. 1C). All the mesenchymal genes examined (*Pax2*, *Lim1*, *Eya1*, *Sall1*, *WT1*, *Hoxa11*, *Gdnf*, integrin α8, integrin α3, *Ncam*, E-cadherin and K-cadherin) were expressed, and the expression continued to day 20 (Fig. 1C, lanes 3-5). By contrast, when cultured on 3T3*lacZ*, the expression of these genes was below the detection level (lanes 7-9). The expression of ureteric bud markers (*Ret* and *Hoxb7*) were not detected in mesenchyme separated from ureteric bud, suggesting that the separation was successful (lane 1). To determine the potential for differentiation within the colonies, markers for terminally differentiated epithelia in glomeruli (podocyte), proximal or distal tubules, and the loop of Henle were also examined (glomeruli: α-actinin-4, *CD2-AP*, P-cadherin, podoplanin and podocalyxin; proximal tubule: *Aqp1*, *Clc5*, cubilin, megalin and *Sglt1*; Henle's loop: *Brn1* and *Nkcc2*; Henle's loop or distal tubule: *Clck2*, polycystin 2, and *Romk2*; distal tubule: *ENaC*, Na/Ca exchanger and polycystin 1. These markers encode: (1) cytoskeletal or structural proteins: α-actinin-4, *CD2-AP*, P-cadherin, podoplanin and podocalyxin; (2) transcription factor: *Brn1*; (3) water or ion channels: *Aqp1*, *Clc5*, *Clck2*, *Romk2*, *ENaC*, and polycystin1 and 2; and (4) transporters: cubilin, megalin, *Sglt1*, *Nkcc2* and Na/Ca exchanger. As shown in Fig. 1C, almost all the genes examined were expressed at day 20 on 3T3Wnt4 (lane 5), while these markers were not expressed on 3T3*lacZ* (lanes 7-9). To ascertain that these genes were expressed by the colony-forming cells, colonies were formed from GFP transgenic mesenchyme, and cells expressing GFP were separated from feeder layers by using flow cytometry sorting. RT-PCR using RNA from these cells suggested that the marker genes examined were indeed expressed by colony-forming cells (lane 10). Furthermore, we made use of immunocytochemistry and found that Pax2 (Fig. 1D-F), E-cadherin (Fig. 1G-I), Sall1 (Fig. 1J,K), and Aqp1 (Fig. 1L,M) were expressed on colonies. The expression of Pax2 and E-cadherin was not detected on immunocytochemistry at day 3, and was subsequently upregulated by day 10, which was consistent with the result of RT-PCR (Fig. 1D,E,G,H). These data suggest that dissociated cells from the metanephric mesenchyme form colonies on 3T3Wnt4 feeder cells in serum-free conditions, and that these colonies contain differentiated epithelia expressing marker genes for epithelia in glomeruli (podocyte), proximal or distal tubules, and the loop of Henle.

Colonies are derived from a single multipotent renal progenitor

To confirm that these colonies were derived from a single cell, each single cell sorted from the EGFP transgenic mesenchyme was cultured in an individual well of 96-well plates coated with 3T3Wnt4. The sheet-like colony was found in 166 wells out of a total of 1632 (10.2%) from three independent experiments (Fig. 2A).

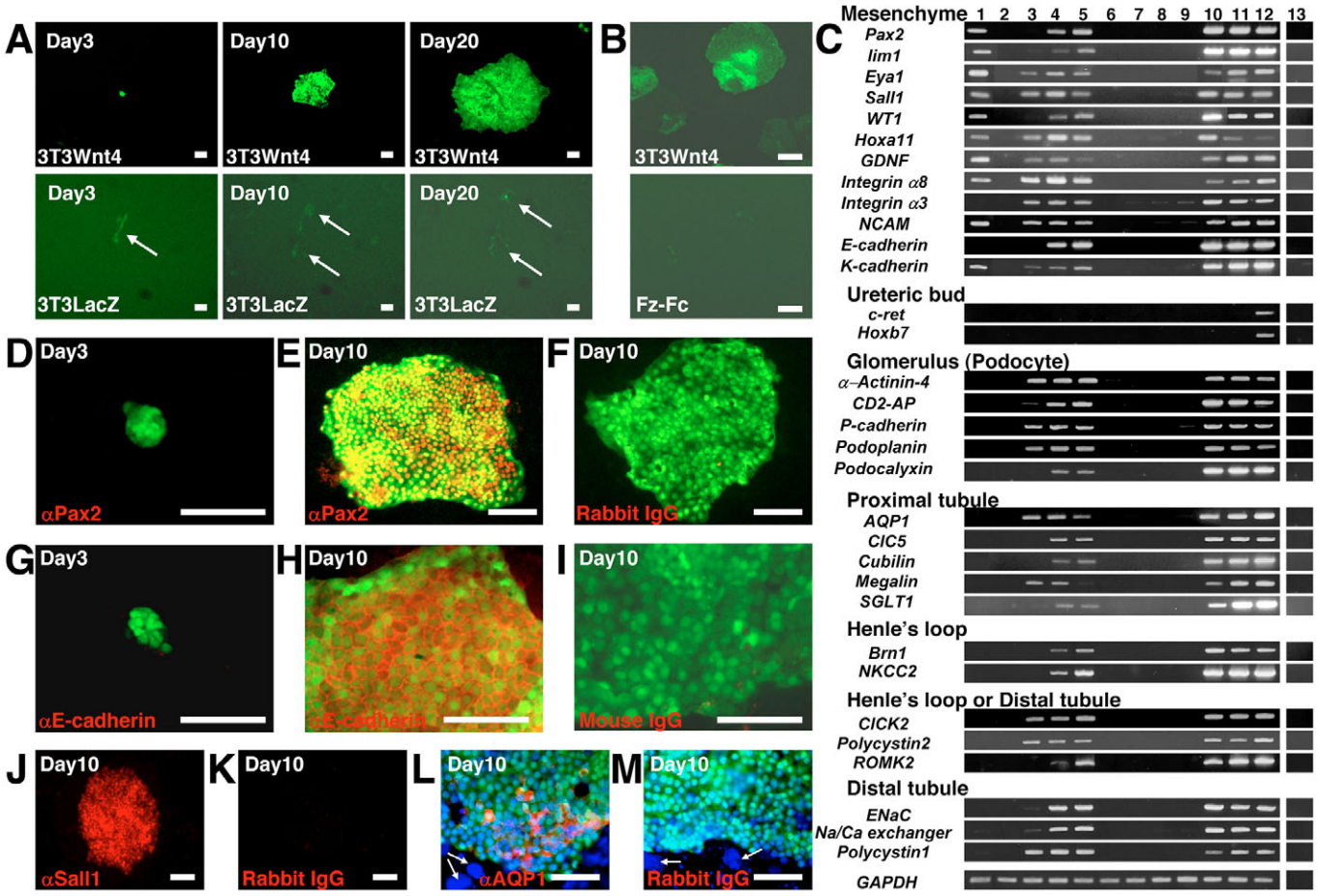

Fig. 1. In vitro colony formation from E11.5 metanephric mesenchyme. (**A**) Sheet-like colonies were formed on 3T3Wnt4, but not on 3T3*lacZ*. Arrows: fibroblast-like cells. (**B**) Colonies were not formed on 3T3Wnt4 with the addition of Fz-Fc chimeric protein. (**C**) RT-PCR analyses of genes expressed in metanephros and fully differentiated epithelia in glomeruli (podocyte), proximal and distal tubules, and the loop of Henle. Lane 1: E11.5 metanephric mesenchyme; 2: 3T3Wnt4 alone; 3: mesenchyme-derived cells cultured on 3T3Wnt4 at day 3; 4: at day 10; 5: at day 20; 6: 3T3*lacZ* alone; 7: mesenchyme-derived cells cultured on 3T3*lacZ* at day 3, 8: at day 10, 9: at day 20, 10: mesenchyme-derived cells at day 10 separated from 3T3Wnt4 feeder cells; 11: organ culture of E11.5 mesenchyme rudiments at day 10; 12: embryonic kidney (E17.5); 13: no RT reaction on mesenchyme-derived cells cultured on 3T3Wnt4 at day 10. (**D**-**M**) Immunocytochemistry of colonies for Pax2 (D-F), E-cadherin (G-I), Sall1 (J,K) and Aqp1 (L,M). (D-I) The expression of Pax2 and E-cadherin (red) was not detected at day 3 (D,G, respectively) but was observed at day 10 (E,H). (J,K) Sall1 expression (red) at day 10. (L,M) Aqp1 (red, proximal tubule marker) was expressed in some cells of the colony. Feeder cells have larger nuclei (DAPI, blue; arrows) than cells consisting of colonies. Control staining with rabbit (F,K,M) and mouse (I) IgGs. Mesenchyme of *Sall1-GFP* knock-in mice was used for J and K to visualize Sall1 expression using anti-GFP immunostaining, while EGFP transgenic mesenchyme was used for D-I,L,M. Scale bars: 50 μm.

To examine the multilineage differentiation of single cell-derived colonies, RT-PCR was done for 22 independent wells containing a colony at day 20. The representative data from three colonies are shown in Fig. 2B (lanes 1-3). Although variation existed between colonies, all the colonies expressed markers for each of the three segments: glomerular podocytes, proximal tubules and Henle's loop or distal tubules. Double staining using PNA and LTL, specific to glomerular podocytes and the proximal renal tubule, respectively, showed that adult kidney (8 weeks old) contained three kinds of cells; single-positive for PNA (those in the glomerulus); single-positive for LTL (those in the proximal renal tubule); and double-negative for LTL or PNA (Fig. 2C, left panel). Similarly, a single cell-derived colony at day 20 contained these three kinds of cells (Fig. 2C, right panel). With a combination of LTL and E-cadherin, at least three cell types were observed in adult kidney (Fig. 2D, left panel) and in a single cell-derived colony (right panel): cells strongly expressing only E-cadherin characteristic of distal renal tubules (Fig. 2D, arrows), and LTL-positive or -negative cells, with a faint expression of E-cadherin in the cell boundary. These results suggest that a colony was derived from a single progenitor, with multipotent differentiating capacity into epithelial cells in glomeruli, proximal and distal tubule, and the loop of Henle.

Colony-forming progenitors exist in the Sall1-GFP^{high} subpopulation of the metanephros

We next attempted to identify prospectively the renal progenitor cells using *Sall1-GFP* knock-in mice (Takasato et al., 2004). As *Sall1* is expressed in mesenchyme-derived tissues, GFP was detected in the mesenchyme around the ureteric bud at E11.5 in the *Sall1-GFP* heterozygous mouse (Fig. 3A, arrows). At E17.5, GFP-expressing cells were observed in the mesenchyme near the surface, as well as in C- or S-shaped bodies, and parts of renal tubules (Fig. 3B). By flow-cytometrical analysis, three subpopulations were fractionated based on the expression of Sall1-GFP: Sall1-GFP^{high},

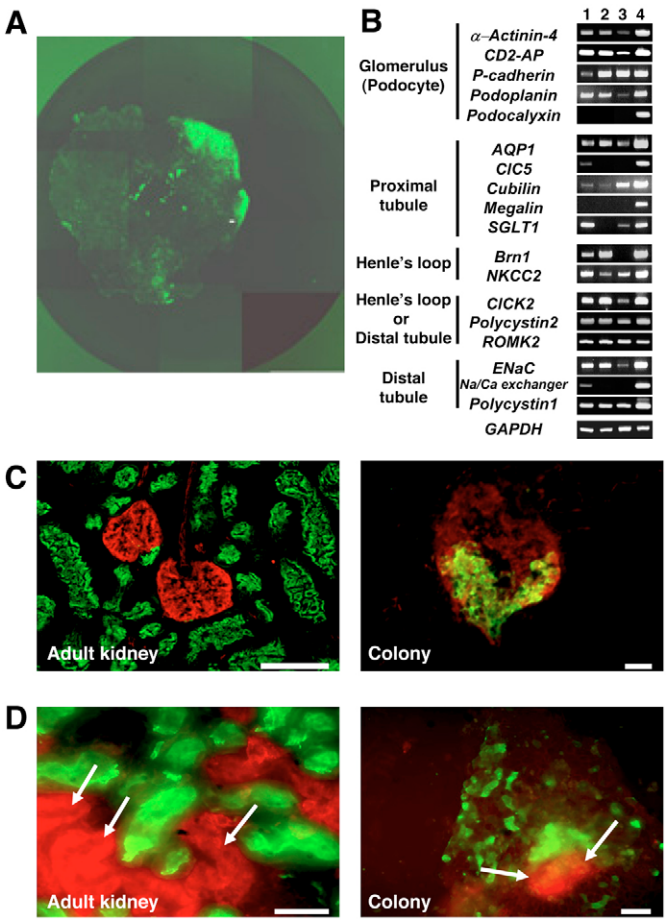

Fig. 2. Colonies are derived from a single multipotent renal progenitor. (**A**) One colony derived from a single cell of EGFP transgenic mesenchyme at culture day 20. (**B**) RT-PCR of three independent wells containing a single cell-derived colony after 20-day culture. Lanes 1-3: colonies; 4: organ culture of E11.5 mesenchyme rudiments. (**C**) Lectin staining of 8-week-old adult kidney (left panel) and a single cell-derived colony (right) with PNA (red, podocyte marker) and with LTL (green, proximal tubule marker). (**D**) Staining of adult kidney (left panel) and a single cell-derived colony (right) with E-cadherin (red, arrow, distal tubule marker) and with LTL (green). Scale bars: 50 μm.

Sall1-GFP^{low} and Sall1-GFP^{negative} (Fig. 3C), and cells in these subpopulations were separated by flow cytometry sorting to be characterized using RT-PCR. As shown in Fig. 3D, Sall1-GFP^{high} cells expressed *Sall1* and *Pax2*. Sall1-GFP^{low} cells expressed markers of stroma (*Foxd1*, previously known as *BF2*), endothelia (*Flk1* and VE-cadherin), and blood cell (*Cd45*), in addition to *Sall1* and *Pax2*. Sall1-GFP^{negative} cells expressed *Flk1* and *Cd45*. The markers of fully differentiated renal epithelia were not expressed in these three populations. These data suggested that cells of stromal lineage were included in cell populations weakly expressing *Sall1* and that those of hemangiogenic lineage were included in both Sall1-GFP^{low} and Sall1-GFP^{negative} populations. Then, the numbers of the colony-forming progenitors in each subpopulation were examined using the low-density culture on 3T3Wnt4 (Fig. 3E). At E11.5, colonies were formed exclusively from the Sall1-GFP^{high} population, and not from Sall1-GFP^{low} or Sall1-GFP^{negative} populations. At E14.5 and 17.5, colonies were also formed only from Sall1-GFP ^{high} subpopulations, but the frequency of colony-forming progenitors decreased as gestation proceeded. These results indicate that renal progenitors with multipotent differentiating capacity are included in cell populations strongly expressing *Sall1* throughout gestation periods.

Sall1-GFP^{high} mesenchyme reconstitutes a three-dimensional structure in organ culture

We next examined the in vitro differentiation capacity of three subpopulations in E11.5 mesenchyme by modifying organ culture of mesenchyme rudiments (Grobstein, 1953; Kispert et al., 1998). Sall1-GFP^{high}, Sall1-GFP^{low} and Sall1-GFP^{negative} cells were separated by flow cytometry, aggregated to form a cell pellet by centrifugation and cultured on 3T3Wnt4 feeder cells in an organ culture setting. Starting from day 3 in culture, tubulogenesis was observed only in the aggregate of the Sall1-GFP^{high} population (Fig. 4A, upper panels), while that from Sall1-GFP^{low} or Sall1-GFP^{negative} did not differentiate and disappeared by day 7 (Fig. 4A, lower panels; data of Sall1-GFP^{negative}, not shown). In sections of the Sall1-GFP^{high} aggregate (Fig. 4B), many tubule- (t) and glomerulus-like structures (g) were observed, and the expression of markers for glomerular podocyte (Wt1, Fig. 1C, red) and proximal tubule (LTL, green) was confirmed by confocal microscopy. These data suggest that only Sall1-GFP^{high} cells differentiate into renal epithelia in vitro in a three-dimensional setting, in addition to forming colonies.

Colony size is affected by the absence of *Sall1*

To investigate the role of *Sall1* in colony formation, mesenchymal cells from *Sall1*$^{+/+}$, *Sall1*$^{+/–}$ and *Sall1*$^{–/–}$ embryos at E11.5, which were obtained from intercrosses of *Sall1-GFP* mice, were plated on 3T3Wnt4 feeder cells at a low density. Ten days after culture, double immunostaining using anti-GFP and anti-E-cadherin antibodies was done to strengthen the green fluorescence and to examine the expression of E-cadherin, respectively (Fig. 5). The numbers of colonies formed were not significantly different among wild-type, heterozygous and homozygous mesenchyme, suggesting that colony-forming progenitors do exist and are not decreased in the absence of *Sall1* (data not shown). Colonies derived from *Sall1*$^{+/+}$ wild-type mesenchyme were not stained with GFP (Fig. 5A), while *Sall1*$^{+/–}$ and *Sall1*$^{–/–}$ colonies were positive for GFP (Fig. 5C,E, green), indicating that *Sall1* itself is not required for *Sall1* promoter activity. Colonies from all three groups (*Sall1*$^{+/+}$, *Sall1*$^{+/–}$ and *Sall1*$^{–/–}$) were also positive for E-cadherin (Fig. 5B,D,F), suggesting that differentiation (mesenchymal-to-epithelial transformation) may not be impaired in the absence of *Sall1*. Indeed, marker gene expression for terminally differentiated epithelia in glomeruli and renal tubules was not changed among *Sall1*$^{+/+}$, *Sall1*$^{+/–}$ and *Sall1*$^{–/–}$ colonies on RT-PCR analyses (data not shown). By contrast, the size of *Sall1*$^{–/–}$ colonies (Fig. 5E,F) was significantly smaller than *Sall1*$^{+/+}$ and *Sall1*$^{+/–}$ colonies (Fig. 5B-D), and this was confirmed statistically (Table 1). Thus, *Sall1* is not

Table 1. Colonies derived from *Sall1*-mutant metanephric mesenchyme

Genotype	Embryos*	Area at day 10 (mean±s.d.) (μm^2) (*n*=60)	*P*
+/+	2	16,118±7219	
+/–	2	16,318±7473	0.44
–/–	2	5140±2071	<0.001

*Number of embryos examined. *P* values were analyzed against wild type (+/+) using a *t*-test. Embryos of a total of four litters were analyzed in this way. Representative data from one experiment are shown.

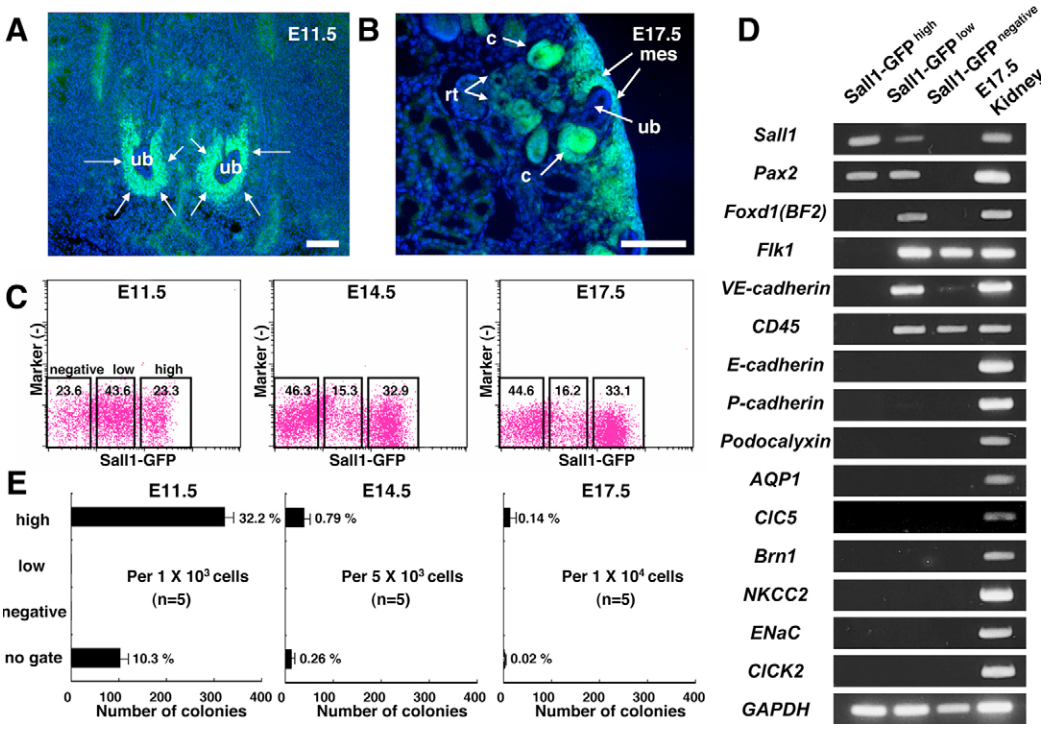

Fig. 3. Colony-forming progenitors exist in the Sall1-GFP^{high} subpopulation of the metanephros. (**A**,**B**) Cryosections of metanephros of *Sall1-GFP* knock-in mouse (A: E11.5; B: E17.5). Blue: DAPI. (**C**) Metanephros contains three subpopulations (Sall1-GFP^{high}, Sall1-GFP^{low} and Sall1-GFP^{negative}). The percentages of the subpopulations at each fetal stage are shown. Figures are the average of five independent experiments. (**D**) RT-PCR analysis of three subpopulations included in E11.5 mesenchyme. (**E**) Numbers of colonies in each subpopulation derived from E11.5 mesenchyme, E14.5 and E17.5 metanephros. The numbers of colony were counted after 20-day culture. The graph shows the average of five independent experiments. ub, ureteric bud; mes, mesenchyme; c, C-shaped body; rt, renal tubule. Scale bars: 50 μm.

required for generation or differentiation of renal progenitors, but the colony size is affected by *Sall1* absence. This is consistent with our previous report that *Sall1*-deficient mesenchyme is competent with respect to epithelial differentiation tested by spinal cord recombination (Nishinakamura et al., 2001). In the spinal cord recombination experiments, *Sall1*-deficient mesenchyme was consistently smaller than wild-type mesenchyme, but this could be due to differences in the initial size of the mesenchyme. Using the colony-forming assay starting from a single cell, we now show that *Sall1* is indeed required for the colony from the mesenchyme to develop into a normal size.

The PCP pathway regulates colony size and the differentiation of colony-forming cells

By combining the colony-forming assay set up in this study and gene transfer using retroviral vector *pMY-IRES-EGFP* (Morita et al., 2000; Kitamura et al., 2003), we observed EGFP expression in 12.9% of colony-forming progenitor cells (116 colonies expressing green fluorescence per total of 896 colonies formed from three independent experiments). Thus, the colony-forming assay in this study enables us to investigate direct effects of reagents and gene transduction on colony-forming progenitor cells, allowing us to examine the roles of Wnt and its downstream branches in kidney development. Positive immunostaining of the colonies for activated JNK1 and 2 indicated that the JNK branch of the PCP pathways (Boutros et al., 1998) may be activated downstream of Wnt4 (Fig. 6A). Indeed, the addition of two kinds of JNK inhibitor (JNKI1 and JNKI2) (Bonny et al., 2001; Bennett et al., 2001) gave rise to smaller colonies than did the control without reagents (Fig. 6B,C, colonies from EGFP transgenic mesenchyme, Table 2). The result of control experiments using the HIV-TAT peptide excluded the possibility that the effects of JNKI1 were derived from non-specific toxicity of the peptide constituting the inhibitor (Fig. 6B). We then investigated effects of both activation and inactivation of Rac1, one of the Rho family GTPases implicated in PCP pathways (Habas et al., 2003), on colony formation. Cells from wild-type E11.5 mesenchyme were transduced with both constitutively active (CA) and dominant-negative (DN) forms of *Rac1* using the retroviral vector *pMY-IRES-EGFP*. Colonies consisting of cells expressing both EGFP and CA-Rac1 were larger than those transduced with *pMY-IRES-EGFP* controls (Fig. 6D, Table 3), suggesting positive effects on colony size. By contrast, the transduction of DN-*Rac1* gave rise to smaller

Table 2. Effects of reagents on the area of colony

Reagent	*n*	Area at day 10 (mean±s.d.) (μm^2)	*P*
Control (without reagents)	20	35,429±15,132	
HIV-TAT peptide	20	38,198±11,357	0.25
JNK inhibitor 1	20	7771±4520	<0.001
Control (without reagents)	30	36,330±15,065	
JNK inhibitor 2	20	6687±2834	<0.001
Y27,632	20	92,359±24,768	<0.001
LiCl	20	5687±3535	<0.001
BIO	30	7436±4897	<0.001
Dkk-1	20	31,998±12,566	0.147

n, number of colonies measured. *P* values were analyzed against control using a *t*-test. For each reagent, more than three independent experiments were performed. Representative data from one experiment are shown.

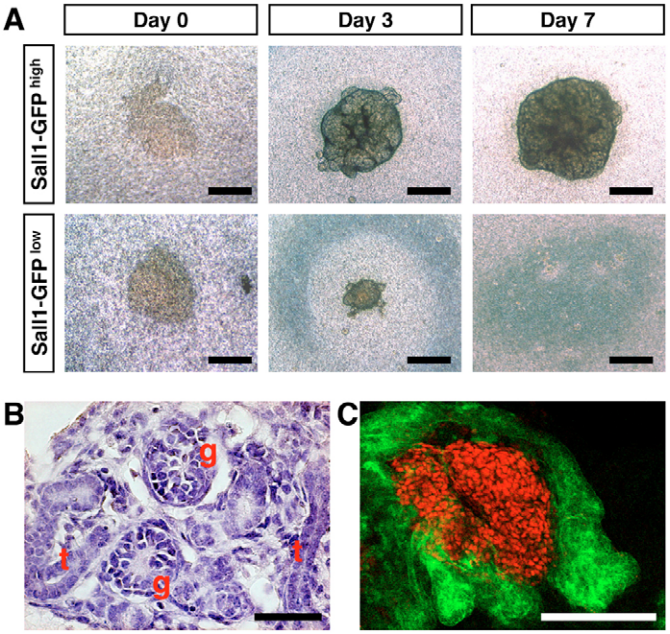

Fig. 4. Sall1-GFP^{high} mesenchyme differentiates into renal epithelia in organ culture. (**A**) Three subpopulations in E11.5 mesenchyme (Sall1-GFP^{high}, Sall1-GFP^{low} and Sall1-GFP^{negative}) were cultured on 3T3Wnt4 feeder cells in an organ culture setting. Only Sall1-GFP^{high} cells (upper panels) differentiated into kidney structure, while Sall1-GFP^{low} cells (lower) disappeared. (**B**) Hematoxylin-eosin staining of sections of Sall1-GFP^{high} aggregates at day 10. Tubule- and glomerulus-like structures are seen. (**C**) Double staining with Wt1 (red, podocyte marker) and LTL (green, proximal tubule marker) of Sall1-GFP^{high} aggregates. g, glomerulus-like structure; t, tubule-like structure. Scale bars: 500 μm in A; 25 μm in B,C.

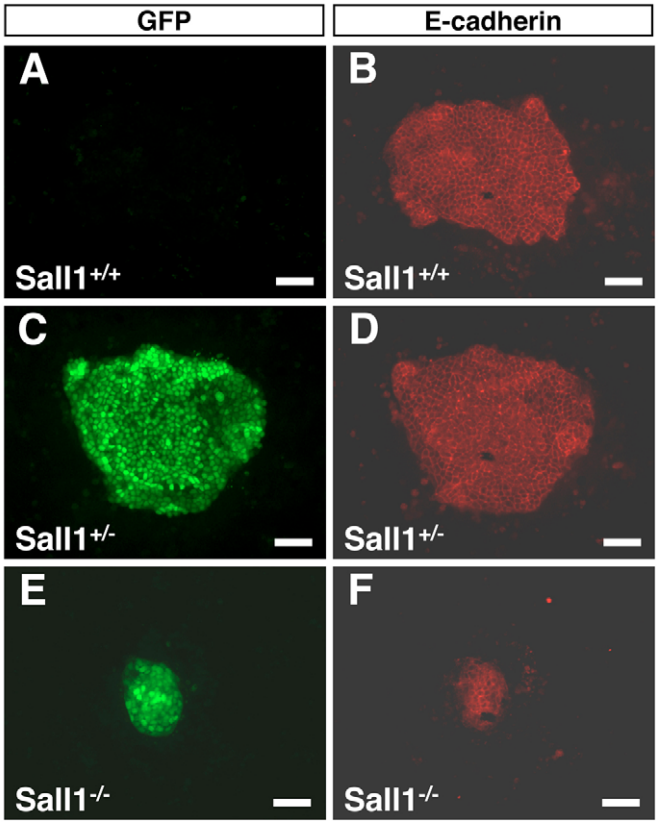

Fig. 5. Colony formation from *Sall1*-mutant metanephric mesenchyme obtained from intercrosses of *Sall1-GFP* mice. (**A-F**) Colonies derived from *Sall1*$^{+/+}$ (A,B), *Sall1*$^{+/-}$ (C,D) and *Sall1*$^{-/-}$ (E,F) mesenchyme were stained both with anti-GFP (A,C,E, green) and with anti-E-cadherin antibodies (B,D,F, red). *Sall1*-deficient colonies (E,F) were significantly smaller than those from wild-type (A,B) and heterozygous (C,D) mesenchyme. Scale bars: 50 μm.

colonies than did the controls (Fig. 6D, Table 3). The numbers of colonies formed were not significantly changed either with the addition of inhibitors or with gene transduction (data not shown). These data indicate that Rac and JNK pathways positively regulate colony size.

By contrast, inactivation of the Rho/Rho-associated protein kinase (ROCK) pathway, another branch of PCP (Strutt et al., 1997; Winter et al., 2001; Habas et al., 2001; Habas et al., 2003), with the addition of ROCK inhibitor, Y27,632 (Uehata et al., 1997) (Fig. 6E, colonies from EGFP transgenic mesenchyme, Table 2), or the transduction of DN-*RhoA*, increased the colony size (Fig. 6F, Table 3), while the activation with CA-*RhoA* decreased it (Fig. 6F, Table 3). Activation of β-catenin signaling both with the addition of two kinds of glycogen synthetase kinase (GSK)-3 inhibitors, lithium chloride (LiCl) (Klein and Melton, 1996) (Fig. 6G, colonies from EGFP transgenic mesenchyme, Table 2) and (2′Z, 3′E)-6-Bromoindirubin-3′-oxime (BIO) (Sato et al., 2004) (Table 2) and with the transduction of the active form of *β-catenin* (Fig. 6H, Table 3) gave rise to smaller colonies. However, inactivation of the β-catenin pathway with the addition of recombinant dickkopf homolog 1 (Dkk-1), a specific inhibitor of the β-catenin pathway (Glinka et al., 1998) and with the transduction of axin (Zeng et al., 1997) exerted no significant effects on colony formation (Tables 2, 3). These data suggest inhibitory roles of Rho/ROCK and β-catenin pathways in regulating colony size.

RT-PCR analysis showed that the expression of marker genes (E-cadherin, P-cadherin, podocalyxin, *Aqp1, Clc5, Brn1*, *Nkcc2, ENaC* and *Clck2*) was inhibited with the addition of JNK inhibitors (Fig. 6I). Although the addition of LiCl and JNK inhibitors resulted in a decreased size of colonies to the same extent, immunostaining confirmed that E-cadherin was lost with JNK inhibitors 1 and 2, but not with LiCl (Fig. 6J, colonies from EGFP transgenic mesenchyme). Thus, the JNK pathway is likely not only to regulate colony size but also to be involved in epithelialization (mesenchymal-to-epithelial transformation) of colony-forming progenitors.

Table 3. Effects of gene transduction on the area of colony

Gene transduced	*n*	Area at day 20 (mean±s.d.) (μm^2)	*P*
Control (vector)	23	49,666±32,111	
CA-*Rac1*	12	83,990±52,619	0.01
DN-*Rac1*	24	23,045±22,791	<0.001
CA-*RhoA*	12	25,658±19,205	<0.005
DN-*RhoA*	21	89,723±49,989	0.001
Control (vector)	38	62,013±31,212	
Active-*β-catenin*	20	23,241±21,685	<0.001
Axin	22	65,352±27,675	0.34

n, number of colonies measured. *P* values were analyzed against control using a *t*-test. Data from three independent experiments is shown.

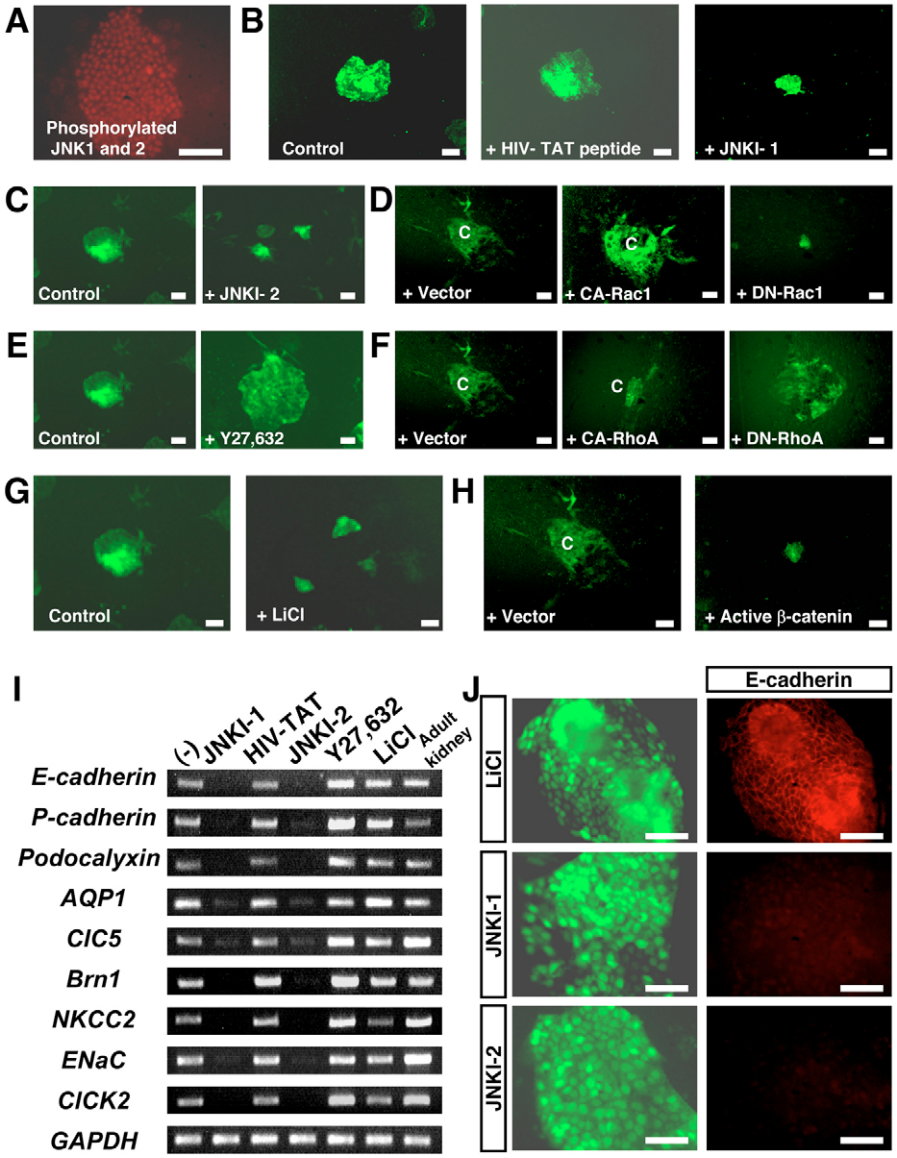

Fig. 6. PCP pathways regulate colony size and the differentiation of colony-forming cells. (**A**) Immunostaining of activated JNK1 and 2 in the colony. (**B**,**C**) The addition of two kinds of JNK inhibitors (JNKI1 and JNKI2, 10 μmol/l) gave rise to smaller colonies than did the control without reagents or HIV-TAT peptide (10 μmol/l). (**D**) The transduction of CA-*Rac1* resulted in an increase in colony size, whereas that of DN-*Rac1* resulted in a decrease. (**E**,**F**) The addition of Y27,632 (E, 10 μmol/l), or the transduction of DN-*RhoA*, increased colony size, while activation with CA-*RhoA* decreased it (F). (**G**,**H**) Activation of the β-catenin pathway by adding LiCl (G, 10 μmol/l) or transducing the active form of *β-catenin* (H) gave rise to smaller colonies. (**I**) RT-PCR analysis of colonies treated with JNKI-1, HIV-TAT peptide, JNKI-2, Y27,632 and LiCl. (**J**) E-cadherin expression was lost with JNKI-1 and -2 but not with LiCl. EGFP transgenic mesenchyme was used for B,C,E,G and J, while wild type was used for D,F and H, to visualize colonies infected by retrovirus vectors. c, colony. Scale bars: 50 μm.

The PCP pathway is involved in tubulogenesis in organ culture

To examine if the results described above were consistent with kidney formation in vivo, we tested the effect of the reagents on whole metanephroi (Fig. 7A-E) and mesenchyme rudiments (F-J) in an organ culture setting. After 7 days of culture, the size of kidney structures was measured. As compared with the control explants cultured without reagents (Fig. 7A,F), the addition of JNK inhibitor 1 (Fig. 7B,G) and JNK inhibitor 2 (Fig. 7C,H) and LiCl (Fig. 7E,J) resulted in a decrease in the size of kidney structures developed, while the addition of ROCK inhibitor Y27,632 (Fig. 7D,I) gave rise to larger ones. These findings were observed both in whole kidney and in mesenchyme rudiments, and were confirmed statistically (Table 4). We also evaluated the effect of the reagents on tubule formation and branching of ureteric bud by staining with an antibody against secreted frizzled-related

Table 4. Effects of reagents on the area of organ culture

	Whole metanephroi			Mesenchymal rudiments		
Reagent	*n*	Area at day 7 (mean ± s.d.) (mm^2)	*P*	*n*	Area at day 7 (mean ± s.d.) (mm^2)	*P*
Control (without reagents)	7	1.717±0.381		6	1.912±0.200	
HIV-TAT peptide	5	1.500±0.215	0.12	7	1.838±0.364	0.33
JNK inhibitor 1	6	1.020±0.325	<0.005	7	0.651±0.131	<0.001
JNK inhibitor 2	6	1.105±0.260	<0.005	7	1.078±0.377	<0.001
Y27,632	5	2.871±0.879	<0.01	7	3.401±0.433	<0.001
LiCl	5	0.716±0.070	<0.001	7	1.270±0.238	<0.001

n, number of explants measured. *P* values were analyzed against control by using a *t*-test. Data from five independent experiments each for whole metanephroi and mesenchyme rudiments are shown.

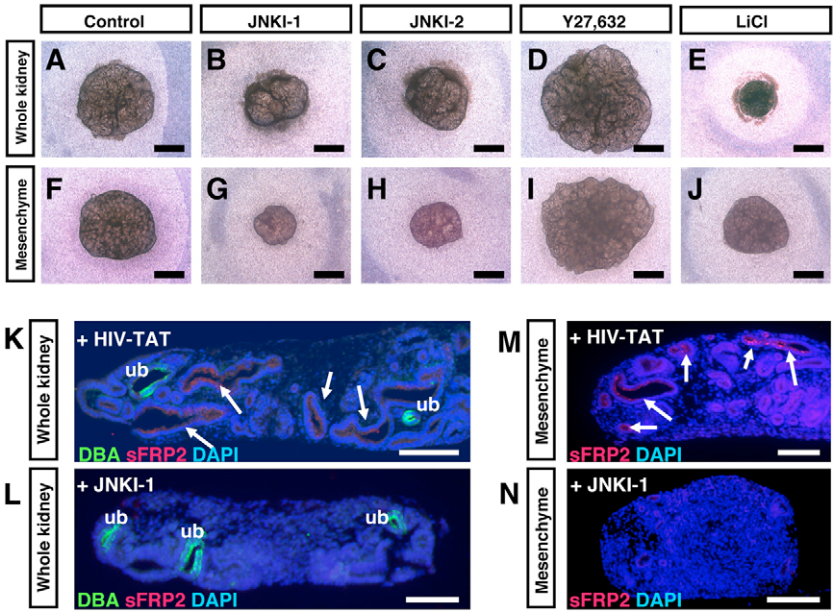

Fig. 7. Effects of reagents on tubulogenesis in organ culture. Whole metanephroi (**A-E**) and mesenchyme rudiments (**F-J**) cultured for 7 days. (A,F) Control explants without reagents, (B,G) 10 μmol/l JNK inhibitor 1 (JNKI1), (C,H) 10 μmol/l JNKI2, (D,I) 10 μmol/l Y27,632, (E,J) 20 mmol/l (E) and 10 mmol/l (J) LiCl. (**K**,**L**) Section staining using DBA (green), an anti-sFRP2 antibody (red) and DAPI (blue) on whole kidneys treated with 15 μmol/l HIV-TAT peptide (K) and JNKI-1 (L). (**M**,**N**) Double labeling with sFRP2 and DAPI on mesenchyme rudiments treated with HIV-TAT peptide (M) and JNKI-1 (N). ub, ureteric bud. Scale bars: 500 μm in A-J; 200 μm in K-N.

protein 2 (sFRP2; Fig. 7K-N, red), the gene expressed only in newly formed tubular epithelia (Lescher et al., 1998), and DBA (Fig. 7K,L, green), respectively. While some tubules expressing sFRP2 were found in explants treated with control HIV-TAT peptide (Fig. 7K,M, arrows), they were lost with JNK inhibitor 1 both in whole metanephroi (Fig. 7L) and in mesenchyme explants (Fig. 7N), suggesting the involvement of JNK pathways in mesenchymal-to-epithelial transformation in organ culture. By contrast, branching of ureteric bud was proportional to the size of explants, and there were no specific effects of the reagents observed on the ureteric bud itself (data not shown). These findings were consistent with the results observed in the colony-forming assay (Fig. 6, Table 2). Thus our colony-forming assay, which enables analysis at a single cell level, could be used for examining mechanisms of three-dimensional kidney development.

DISCUSSION

Renal progenitors defined by colony-forming assay

In this study, we provide evidence, using in vitro clonal analysis combined with flow cytometry, for the presence of progenitor cells in the fetal mouse kidney. Results of staining with PNA, LTL and E-cadherin, and of RT-PCR showed the differentiating capacity of a single Sall1-GFP^{high} cell into glomerular epithelia (podocyte), proximal and distal tubule, respectively. In addition to lineage-marker expression, both glomerulus- and tubule-like structures were reconstituted by Sall1-GFP^{high} cells, supporting their differentiation ability. A multipotent renal stem cell line has been isolated from E11.5 mesenchyme utilizing immortalization with T antigen of SV40 virus (Oliver et al., 2002). The cell line expresses marker genes of endothelia and smooth muscle cells with treatment of TGFβ1, in addition to gene expression of mesenchyme and renal epithelia. It has not been known, however, whether they normally resided in the fetal kidney or accidentally emerged by the influence of the process with immortalization. In our colony-forming system, gene expression of endothelia and smooth muscle cells was not observed, and expression of *Foxd1* (*BF2*), a marker gene specific to stroma, a third cell population included in metanephros was not found (data not shown). Thus, it remains to be elucidated whether embryonic kidney contains stem cells that can differentiate into endothelium, smooth muscle or stroma in addition to epithelia of glomerulus and renal tubules.

The renal progenitors defined by our colony-forming assay are included in cell populations strongly expressing *Sall1* throughout gestation periods, and they might continue to reside in the outer layer of embryonic kidney, where undifferentiated metanephric mesenchyme resides and strongly expresses *Sall1* (Fig. 3B). As shown in Table 5, the total cell numbers of metanephros increased and the frequency of colony-forming Sall1-GFP^{high} cells decreased as gestation proceeded. Interestingly, the calculated numbers of the colony-forming cells remained almost constant throughout gestation periods (400-800 cells/embryonic kidney). The amplification of these progenitors might not occur in the embryonic kidney. One interesting question is whether they continue to remain in the adult kidney. From 8-week-old mice, however, colonies were not formed under the same culture conditions (data not shown). Renal progenitors defined by our colony-forming assay might be lost by the time kidney development is complete.

Table 5. Calculated number of colony-forming progenitors in embryonic kidney

	E11.5	E14.5	E17.5
Total cell number of kidney (×10^4)	0.77±0.24	21.4±2.7	77.9±19.4
Sall1-GFP^{high} cells in kidney (%)	23.6±1.7	46.3±2.1	44.5±0.9
Colony formation in Sall1-GFP^{high} cells (%)	32.2±2.8	0.79±0.18	0.14±0.07
Calculated numbers of colony-forming cells*	585.1	782.7	485.3

Mean±s.d. (from five independent experiments each for E11.5, E14.5, and E17.5).
*Numbers of colony-forming cells were calculated by multiplying the means of the three values above.

Analysis of gene function in kidney development by colony-forming assay

The knowledge of gene function in kidney development has mainly been obtained from analyses using knockout mice, while experimental systems that investigate gene function in individual cells of metanephros have been lacking. By setting up a novel system combining colony formation from a single cell and gene transduction using a retroviral vector, our culture system enables the direct observation of effects of reagents and gene transduction on colony-forming progenitor cells. As similar results were obtained from organ culture experiments (Fig. 7), it is less likely that the cellular behavior observed in our colony-assay system might be artifactual.

Mice lacking the constituent genes involved in downstream branches of Wnt signaling pathways often show early embryonic lethality, such as *Rac1* (Sugihara et al., 1998), *Jnk1* and *Jnk2* (Kuan et al., 1999), β-catenin (Haegel et al., 1995), axin (Zeng et al., 1997), and their functions in kidney morphogenesis remain largely unknown. Using our culture system, functions of these genes in metanephros development were elucidated. Furthermore, experiments for colony formation from mesenchyme of *Sall1*-mutant embryos demonstrated the roles of *Sall1* for the colony size. Thus, the colony-assay system set up in this study can also be applied to the analysis of genetic mouse models.

Roles of PCP pathway in kidney development

Among downstream branches of Wnt4 signal, we found that Rac- and JNK-dependent PCP pathways positively regulated the colony size and the differentiation of colony-forming cells. This result is compatible with several previous reports (Du et al., 1995; Ungar et al., 1995; Maretto et al., 2003). In frogs and fish, the Wnt4 family does not strongly activate the β-catenin pathway, and affects convergent extension, which is polarized movement during embryonic development regulated by the PCP pathway (Du et al., 1995; Ungar et al., 1995). Activation of the β-catenin signaling was not detected at various stages of differentiation of the metanephric mesenchyme, which was examined using transgenic mice expressing the *lacZ* reporter genes under the control of β-catenin/TCF responsive elements (Maretto et al., 2003). Furthermore, activation of the β-catenin pathway is implicated in epithelial-to-mesenchymal transition during mesoderm formation in embryonic development and tumorigenesis (Polakis, 2000; Bienz and Clevers, 2000), which is opposite to the process we examined in this study: mesenchymal-to-epithelial transformation. Thus it may be possible that PCP pathways, not the β-catenin pathway, play central roles as downstream branches of Wnt4 for epithelial differentiation of metanephric mesenchyme.

We demonstrated that Rac1 and RhoA play positive and negative roles for the regulation of colony size, respectively. The Rho family of small GTPases is known to be implicated in cell proliferation by the regulation of cell cycle progression, in addition to its effects on the cytoskeleton (Etienne-Manneville and Hall, 2002). Antagonism, or the opposing activities, between two Rho GTPases have been noted in some cell types (Luo, 2000; Gu et al., 2005). For instance, a hematopoietic-specific Rho GTPase, RhoH, negatively regulates both growth and actin-based function of hematopoietic progenitors via suppression of Rac-mediated signaling (Gu et al., 2005). Similarly, our data suggested the possibility that Rac1 and RhoA might antagonistically regulate the growth of progenitors in kidney development. Recently the roles of the JNK pathway in epithelial morphogenesis have been noted both in *Drosophila* and in mice (Xia and Karin, 2004). Our data also suggested the essential roles of JNK pathways in epithelialization, as well as in regulation of colony size. Common mechanisms regulating epithelial morphogenesis might underlie these processes. The PCP pathways, including the Rho family of small GTPases and JNK, control several developmental processes, mainly by regulating cell cytoskeletons, such as the polarity of hairs on the epidermal cells of *Drosophila* wings, the arrangement of ommatidial cells of *Drosophila* eyes, the polarity of stereocilia in the inner ears of mammals, and convergent extension in *Xenopus* and zebrafish (Veeman et al., 2003; Wallingford et al., 2002). In addition to these processes, we provide a novel hypothesis of the involvement of the PCP pathways in kidney development.

In summary, we set up a novel colony-forming assay by which we demonstrated the presence and the frequency of multipotent progenitor cells in embryonic kidneys. This assay would serve as a useful tool for analyzing differentiation mechanisms in the kidney at a single cell level, taking advantage of the facility of gene transfer.

We thank Dr M. Okabe for providing EGFP transgenic mice, Dr A. Kikuchi for *pBSKS-rAxin*, Dr A. Nagafuchi for *pUC-EF-1α-β-catenin^{SA}-3HA*, Dr H. Koide for *pCAGIP-flag-Rac1* and *RhoA*, Dr T. Kitamura for *pMY-IRES-EGFP* and PLAT-E, Y. Morita for technical support for FACS, and Dr C. Kobayashi for critically reading the manuscript. This work was partly supported by the Ministry of Health, Labor, and Welfare of Japan.

References

Barasch, J., Yang, J., Ware, C. B., Taga, T., Yoshida, K., Erdjument-Bromage, H., Tempst, P., Parravicini, E., Malach, S., Aranoff, T. et al. (1999). Mesenchymal to epithelial conversion in rat metanephros is induced by LIF. *Cell* **99**, 377-386.

Bennett, B. L., Sasaki, D. T., Murray, B. W., O'Leary, E. C., Sakata, S. T., Xu, W., Leisten, J. C., Motiwala, A., Pierce, S., Satoh, Y. et al. (2001). SP600125, an anthrapyrazolone inhibitor of Jun N-terminal kinase. *Proc. Natl. Acad. Sci. USA* **98**, 13681-13686.

Bienz, M. and Clevers, H. (2000). Linking colorectal cancer to Wnt signaling. *Cell* **103**, 311-320.

Bonny, C., Oberson, A., Negri, S., Sauser, C. and Schorderet, D. F. (2001). Cell-permeable peptide inhibitors of JNK: novel blockers of beta-cell death. *Diabetes* **50**, 77-82.

Boutros, M., Paricio, N., Strutt, D. I. and Mlodzik, M. (1998). Dishevelled activates JNK and discriminates between JNK pathways in planar polarity and Wingless signaling. *Cell* **94**, 109-118.

Bradley, T. R. and Metcalf, D. (1966). The growth of mouse bone marrow cells in vitro. *Aust. J. Exp. Biol. Med. Sci.* **44**, 287-299.

Carroll, T. J., Park, J. S., Hayashi, S., Majumdar, A. and McMahon, A. P. (2005). Wnt9b plays a central role in the regulation of mesenchymal to epithelial transitions underlying organogenesis of the mammalian urogenital system. *Dev. Cell* **9**, 283-292.

Du, S. J., Purcell, S. M., Christian, J. L., McGrew, L. L. and Moon, R. T. (1995). Identification of distinct classes and functional domains of Wnts through expression of wild-type and chimeric proteins in *Xenopus* embryos. *Mol. Cell. Biol.* **15**, 2625-2634.

Etienne-Manneville, S. and Hall, A. (2002). Rho GTPases in cell biology. *Nature* **420**, 629-635.

Gilbert, T., Gaonach, S., Moreau, E. and Merlet-Benichou, C. (1994). Defect of nephrogenesis induced by gentamicin in rat metanephric organ culture. *Lab. Invest.* **70**, 656-666.

Glinka, A., Wu, W., Delius, H., Monaghan, A. P., Blumenstock, C. and Niehrs, C. (1998). Dickkopf-1 is a member of a new family of secreted proteins and functions in head induction. *Nature* **391**, 357-362.

Grobstein, C. (1953). Inductive epithelio-mesenchymal interaction in cultured organ rudiments of the mouse metanephros. *Science* **118**, 52-55.

Gu, Y., Jasti, A. C., Jansen, M. and Siefring, J. E. (2005). RhoH, a hematopoietic-specific Rho GTPase, regulates proliferation, survival, migration, and engraftment of hematopoietic progenitor cells. *Blood* **105**, 1467-1475.

Habas, R., Kato, Y. and He, X. (2001). Wnt/Frizzled activation of Rho regulates vertebrate gastrulation and requires a novel Formin homology protein Daam1. *Cell* **107**, 843-854.

Habas, R., Dawid, I. B. and He, X. (2003). Coactivation of Rac and Rho by Wnt/Frizzled signaling is required for vertebrate gastrulation. *Genes Dev.* **17**, 295-309.

Haegel, H., Larue, L., Ohsugi, M., Fedorov, L., Herrenknecht, K. and Kemler, R. (1995). Lack of beta-catenin affects mouse development at gastrulation. *Development* **121**, 3529-3537.

Herzlinger, D., Koseki, C., Mikawa, T. and Al-Awqati, Q. (1992). Metanephric mesenchyme contains multipotent stem cells whose fate is restricted after induction. *Development* **114**, 565-572.
Herzlinger, D., Qiao, J., Cohen, D., Ramakrishna, N. and Brown, A. M. C. (1994). Induction of kidney epithelial morphogenesis by cells expressing *Wnt-1*. *Dev. Biol.* **166**, 815-818.
Ikeda, S., Kishida, S., Yamamoto, H., Murai, H., Koyama, S. and Kikuchi, A. (1998). Axin, a negative regulator of the Wnt signaling pathway, forms a complex with GSK-3beta and beta-catenin and promotes GSK-3beta-dependent phosphorylation of beta-catenin. *EMBO J.* **17**, 1371-1384.
Kispert, A., Vainio, S. and McMahon, A. P. (1998). Wnt-4 is a mesenchymal signal for epithelial transformation of metanephric mesenchyme in the developing kidney. *Development* **125**, 4225-4234.
Kitamura, T., Koshino, Y., Shibata, F., Oki, T., Nakajima, H., Nosaka, T. and Kumagai, H. (2003). Retrovirus-mediated gene transfer and expression cloning: powerful tools in functional genomics. *Exp. Hematol.* **31**, 1007-1014.
Klein, P. S. and Melton, D. A. (1996). A molecular mechanism for the effect of lithium on development. *Proc. Natl. Acad. Sci. USA* **93**, 8455-8459.
Kuan, C. Y., Yang, D. D., Samanta Roy, D. R., Davis, R. J., Rakic, P. and Flavell, R. A. (1999). The Jnk1 and Jnk2 protein kinases are required for regional specific apoptosis during early brain development. *Neuron* **22**, 667-676.
Lescher, B., Haenig, B. and Kispert, A. (1998). sFRP-2 is a target of the Wnt-4 signaling pathway in the developing metanephric kidney. *Dev. Dyn.* **213**, 440-451.
Luo, L. (2000). Rho GTPases in neuronal morphogenesis. *Nat. Rev. Neurosci.* **1**, 173-180.
Maretto, S., Cordenonsi, M., Dupont, S., Braghetta, P., Broccoli, V., Hassan, A. B., Volpin, D., Bressan, G. M. and Piccolo, S. (2003). Mapping Wnt/β-catenin signaling during mouse development and in colorectal tumors. *Proc. Natl. Acad. Sci. USA* **100**, 3299-3304.
Miller, J. R., Hocking, A. M., Brown, J. D. and Moon, R. T. (1999). Mechanism and function of signal transduction by the Wnt/β-catenin and Wnt/Ca^{2+} pathways. *Oncogene* **18**, 7860-7872.
Miyagishi, M., Fujii, R., Hatta, M., Yoshida, E., Araya, N., Nagafuchi, A., Ishihara, S., Nakajima, T. and Fukamizu, A. (2000). Regulation of Lef-mediated transcription and p53-dependent pathway by associating beta-catenin with CBP/p300. *J. Biol. Chem.* **275**, 35170-35175.
Morita, S., Kojima, T. and Kitamura, T. (2000). Plat-E: an efficient and stable system for transient packaging of retroviruses. *Gene Ther.* **7**, 1063-1066.
Nishinakamura, R., Matsumoto, Y., Nakao, K., Nakamura, K., Sato, A., Copeland, N. G., Gilbert, D. J., Jenkins, N. A., Scully, S., Lacey, D. L. et al. (2001). Murine homolog of *SALL1* is essential for ureteric bud invasion in kidney development. *Development* **128**, 3105-3115.
Okabe, M., Ikawa, M., Kominami, K., Nakanishi, T. and Nishimune, Y. (1997). 'Green mice' as a source of ubiquitous green cells. *FEBS Lett.* **407**, 313-319.
Oliver, J. A., Barasch, J., Yang, J., Herzlinger, D. and Al-Awqati, Q. (2002). Metanephric mesenchyme contains embryonic renal stem cells. *Am. J. Physiol.* **283**, F799-F809.
Plisov, S. Y., Yoshino, K., Dove, L. F., Higinbotham, K. G., Rubin, J. S. and Perantoni, A. O. (2001). TGFβ2, LIF and FGF2 cooperate to induce nephrogenesis. *Development* **128**, 1045-1057.
Pluznik, D. H. and Sachs, L. (1965). The cloning of normal "mast" cells in tissue culture. *J. Cell Physiol.* **66**, 319-324.
Polakis, P. (2000). Wnt signaling and cancer. *Genes Dev.* **14**, 1837-1851.
Reynolds, B. A., Tetzlaff, W. and Weiss, S. (1992). A multipotent EGF-responsive striatal embryonic progenitor cell produces neurons and astrocytes. *J. Neurosci.* **12**, 4565-4574.
Sato, N., Meijer, L., Skaltsounis, L., Greengard, P. and Brivanlou, A. H. (2004). Maintenance of pluripotency in human and mouse embryonic stem cells through activation of Wnt signaling by a pharmacological GSK-3-specific inhibitor. *Nat. Med.* **10**, 55-63.
Saxen, L. (1987). *Organogenesis of the Kidney*. New York: Cambridge University Press.
Stark, K., Vainio, S., Vassileva, G. and McMahon, A. P. (1994). Epithelial transformation of metanephric mesenchyme in the developing kidney regulated by Wnt-4. *Nature* **372**, 679-683.
Strutt, D. I., Weber, U. and Mlodzik, M. (1997). The role of RhoA in tissue polarity and Frizzled signaling. *Nature* **387**, 292-295.
Sugihara, K., Nakatsuji, N., Nakamura, K., Nakao, K., Hashimoto, R., Otani, H., Sakagami, H., Kondo, H., Nozawa, S., Aiba, A. et al. (1998). Rac1 is required for the formation of three germ layers during gastrulation. *Oncogene* **17**, 3427-3433.
Takasato, M., Osafune, K., Matsumoto, Y., Kataoka, Y., Yoshida, N., Meguro, H., Aburatani, H., Asashima, M. and Nishinakamura, R. (2004). Identification of kidney mesenchymal genes by a combination of microarray analysis and *Sall1-GFP* knockin mice. *Mech. Dev.* **121**, 547-557.
Uehata, M., Ishizaki, T., Satoh, H., Ono, T., Kawahara, T., Morishita, T., Tamakawa, H., Yamagami, K., Inui, J., Maekawa, M. et al. (1997). Calcium sensitization of smooth muscle mediated by a Rho-associated protein kinase in hypertension. *Nature* **389**, 990-994.
Ungar, A. R., Kelly, G. M. and Moon, R. T. (1995). Wnt4 affects morphogenesis when misexpressed in the zebrafish embryo. *Mech. Dev.* **52**, 153-164.
Veeman, M. T., Axelrod, J. D. and Moon, R. T. (2003). A second canon: functions and mechanisms of β-catenin-independent Wnt signaling. *Dev. Cell* **5**, 367-377.
Wallingford, J. B., Fraser, S. E. and Harland, R. M. (2002). Convergent extension: the molecular control of polarized cell movement during embryonic development. *Dev. Cell* **2**, 695-706.
Winter, C. G., Wang, B., Ballew, A., Royou, A., Karess, R., Axelrod, J. D. and Luo, L. (2001). *Drosophila* Rho-associated kinase (Drok) links Frizzled-mediated planar cell polarity signaling to the actin cytoskeleton. *Cell* **105**, 81-91.
Wodarz, A. and Nusse, R. (1998). Mechanisms of Wnt signaling in development. *Annu. Rev. Cell Dev. Biol.* **14**, 59-88.
Xia, Y. and Karin, M. (2004). The control of cell motility and epithelial morphogenesis by Jun kinases. *Trends Cell Biol.* **14**, 94-101.
Zeng, L., Fagotto, F., Zhang, T., Hsu, W., Vasicek, T. J., Perry, W. L., 3rd, Lee, J. J., Tilghman, S. M., Gumbiner, B. M. and Costantini, F. (1997). The mouse Fused locus encodes Axin, an inhibitor of the Wnt signaling pathway that regulates embryonic axis formation. *Cell* **90**, 181-192.